Earth Planets Space, **58**, 1139–1146, 2006

Electron temperature variation associated with the auroral energy input during the DELTA campaign

Takumi Abe, Koh-Ichiro Oyama, and Akihiro Kadohata

Institute of Space and Astronautical Science, Japan Aerospace Exploration Agency, 3-1-1, Yoshinodai, Sagamihara, Kanagawa 229-8510, Japan

(Received October 25, 2005; Revised July 13, 2006; Accepted July 27, 2006; Online published September 29, 2006)

Japanese sounding rocket "S-310-35" was launched from Andøya Rocket Range in Norway on December 13, 2004 during Dynamics and Energetics of the Lower Thermosphere in Aurora (DELTA) campaign, in which the rocket-borne *in-situ* measurements and ground-based measurements were coordinated to conduct a comprehensive observation of the upper atmospheric response against the auroral energy input. The Fast Langmuir Probe (FLP) was installed on the sounding rocket to study thermal structure and energy balance of the plasma by measuring the electron temperature in the polar lower ionosphere. The FLP observations indicate that the electron temperatures were found to be remarkably high in an altitude range from 106 km to 114 km during the ascending phase of the rocket. The lowest part of this high temperature region might be affected by artificial electron beam which was generated by the N_2 temperature instrument on the same rocket. On the other hand, a small increase of the electron temperature was observed at the altitude from 114 to 119 km in the descending phase. This is possibly the first time that both the temperature increase and density fluctuation that may be caused by the Farley-Buneman instability were detected by *in-situ* observation.

Key words: Electron temperature, ionosphere, heating, sounding rocket.

1. Introduction

Langmuir probes have been employed for many years on sounding rockets and satellites to measure the temperature and number density of thermal electrons in the ionospheric plasma. The temperature and density have been extensively measured for studying of the dynamics and energetics, because thermal population is the most important constituent as plasma in the lower ionosphere. The Langmuir probe technique involves measuring the volt-ampere characteristics of one or more bare metal collectors to which a DC bias is applied. Because of its simplicity and convenience, Langmuir probe is one of the instruments that have been installed most frequently on the rocket and satellite. In the Langmuir probe measurement, the accuracy depends primarily on avoiding implementation errors rather than the validity of the Langmuir probe equations for the temperature and density estimates. Brace (1998) discussed the theory of the method, the main sources of error, and some approaches that have been used to reduce the errors.

In general, the thermal structure of the ionosphere is more complex at high latitudes than at lower latitudes because of additional heating processes such as energetic particle precipitation and Joule heating, besides the solar EUV radiation heating. These processes are variable and known to be characterized by the coupling with the magnetospheric phenomena. From many years ago, an influence of these heating on the lower ionosphere has been quantitatively evaluated by theoretical and empirical studies. For example, Banks *et al*. (1974) created a computational model to describe the interaction of auroral electrons with the atmosphere by combining continuous energy losses and small angle deflections in a Fokker-Planck diffusion equation. They calculated the energy deposition rates of secondary electron and degraded primary electron production at all heights. Also, Banks (1977) deduced atmospheric heating rates associated with particle precipitation and Joule dissipation from the Chatanika incoherent radar observations. The calculated altitude profiles of these heat inputs showed that the energy liberated by Joule dissipation tends to peak at a substantially higher altitude (∼130 km) than that due to particles (100–120 km). Brekke (1983) published a short review of different techniques for deriving the amount of heat input into the auroral upper atmosphere due to Joule heating and particle precipitation with a stress in the relative importance and altitude of these two energy sources with respect to auroral substorm time. It was also pointed out that there is still a lack of measurements of enhanced neutral temperatures in the lower thermosphere during auroral disturbances.

In the E region, large electric fields can also lead to anomalous electron temperature owing to the excitation of plasma instabilities. Specifically, in the auroral E region the electrons drift in the $E \times B$ direction, while the ions drift in the E direction. This ion-electron relative drift excites a modified two-stream instability when the electric field exceeds a threshold. The subsequent interaction of the plasma waves and the electrons heats the electron gas (St.-Maurice, 1990).

The thermospheric response to auroral disturbances in meso-scale (1–1000 km) has not been well understood

Table 1. Detailed specification of the FLP instrument.

Sampling	1.25 msec (800 Hz)		
Sweep period	250 msec (Sweep up 125 msec, down 125 msec)		
Sweep voltage	Triangular, 3 Vp-p (with respect to the rocket)		
Current gain		Gain High mode	Gain Low mode
	Low Gain	× 1.0	× 0.5
	Middle Gain	× 20.0	× 10.0
	High Gain	× 400.0	× 200.0
Weight	1.5 kg (FLP-S)		
	1.5 kg (FLP-E)		
	0.25 kg (FLP-PRE)		
Size	255 × 65 × 92.2 H mm (FLP-S)		
	211 ×100 × 60 H mm (FLP-E)		
	126 × 29 × 83 H mm (FLP-PRE)		
Power	255 mA (+18 V)		
	150 mA (−18 V)		

Table 2. Timer sequence for the FLP operation.

Item	Time from launch (sec)	Altitude (km)
FLP-Window Open	63	70.8
FLP-Glass Cut	65	73.0
FLP-Probe Extension	66	74.1
FLP-Gain Down	120	120.7
FLP-Gain Up	259	130.7

while the large-scale circulation in the high latitude thermosphere has been investigated with many modeling studies and from satellite observations. Recent rocket observations in the high latitude thermosphere are mainly concentrated in wind measurements, and thereby strong winds and wind shears are observed in the lower thermosphere (Larsen *et al.*, 1995, 1997). However, a cause of these vertical wind structures is not fully identified mainly because of uncertainty in parameters necessary for the modeling study.

In December 2004, the coordinated sounding rocket and ground-based observations were conducted in Norway, with a main scientific purpose for elucidating the dynamics and energetics in the lower thermosphere associated with the auroral energy input. In this campaign, the instruments on board the rocket successfully performed their measurements, and provided the temperature and density of molecular nitrogen, auroral emission rate, and the ambient plasma parameters, which are inherent for the understanding of upper atmospheric energetics triggered by the auroral energy deposition. The Fast Langmuir Probe (FLP), among 8 rocket-borne instruments (Abe *et al.*, 2006) is supposed to play a role in providing the temperature information of the ionospheric thermal electrons. The electron temperature can be estimated from the Voltage-Current characteristic curve measured by the probe.

The final goal of the FLP observations is to elucidate the energy budget in the lower ionosphere from a viewpoint of the thermal electron temperature measurement during the DELTA campaign. Since thermal electrons in the ionosphere instantaneously responds to various energy input from external sources, it is one of the most important parameter to understand the thermal energy budget in the ionosphere. In this paper, we discuss variations of the electron temperature along the rocket trajectory, as a preliminary report, with a particular interest of the heating processes which are characteristic in the high-latitude lower ionosphere. A quantitative discussion of the energy budget extracted from temperature observations in the lower ionosphere is the important scientific theme, and will be made in the future research.

2. Instrument

The Fast Langmuir Probe (FLP) onboard the sounding rocket "S-310-35" consists of a cylindrical stainless probe with a length of 140 mm and a diameter of 3 mm, and was installed on the payload zone in the direction perpendicular to the rocket spin axis. Detailed specification of the probe is given in Table 1. The probe is directly biased by a triangular voltage with amplitude of 3 V with respect to the rocket potential and a period of 250 msec in order to provide the incident current-voltage relationship. A current incident on the probe was sampled with a rate of 800 Hz, and amplified by three different gains (low, middle, and high) so that it can work in a wide range of the plasma density. In order to measure the ion current as well as the electron current, the amplifier has an offset voltage of +1 V; a positive (>1 V) voltage means the electron current while a negative one does the ion current. The calibration signal is obtained by switching the input from the probe to the resistance once every 30 seconds. The electron temperature and number density can be derived from a relationship between the incident current versus the probe voltage.

In order to avoid undesirable effect of contaminated layer on the probe surface that may cause a hysteresis in the probe current, the cylindrical electrode sealed in the glass tube has been baked at a high temperature of 200°C in a high vacuum ($<10^{-7}$ torr) for more than 24 hours to get outgas from the probe surface, and subsequently tipped off the vacuum system (Oyama and Hirao, 1976). In this way, uncontaminated probe was glass-sealed. The glass was broken by a spring-actuated sharp edge during the rocket flight and removed by a centrifugal force. One second later, the probe was deployed in the direction vertical to the rocket spin axis so that the clean probe surface can be exposed to the plasma outside of the rocket sheath.

Table 2 summarizes a timer sequence prepared for the FLP operation. After 3 seconds from the rocket nose cone was removed, a window for the probe extension was opened, followed by cutting the glass one second later. Then, the probe was deployed perpendicular to the rocket axis. The gain for the current amplifier was switched from high (low) mode to low (high) mode at an altitude of 120.7 (130.7) km during the ascending (descending) flight in order to adjust for the altitudinal variation of the plasma density.

The rocket "S-310-35" carried a suite of 8 instruments to investigate the dynamics and energetics in the lower thermosphere associated with the auroral energy input (Abe *et al.*, 2006). Among them, the N_2 Temperature instrument (NTV) emits the electron beam in order to measure a vibrational temperature, rotational temperature, and number

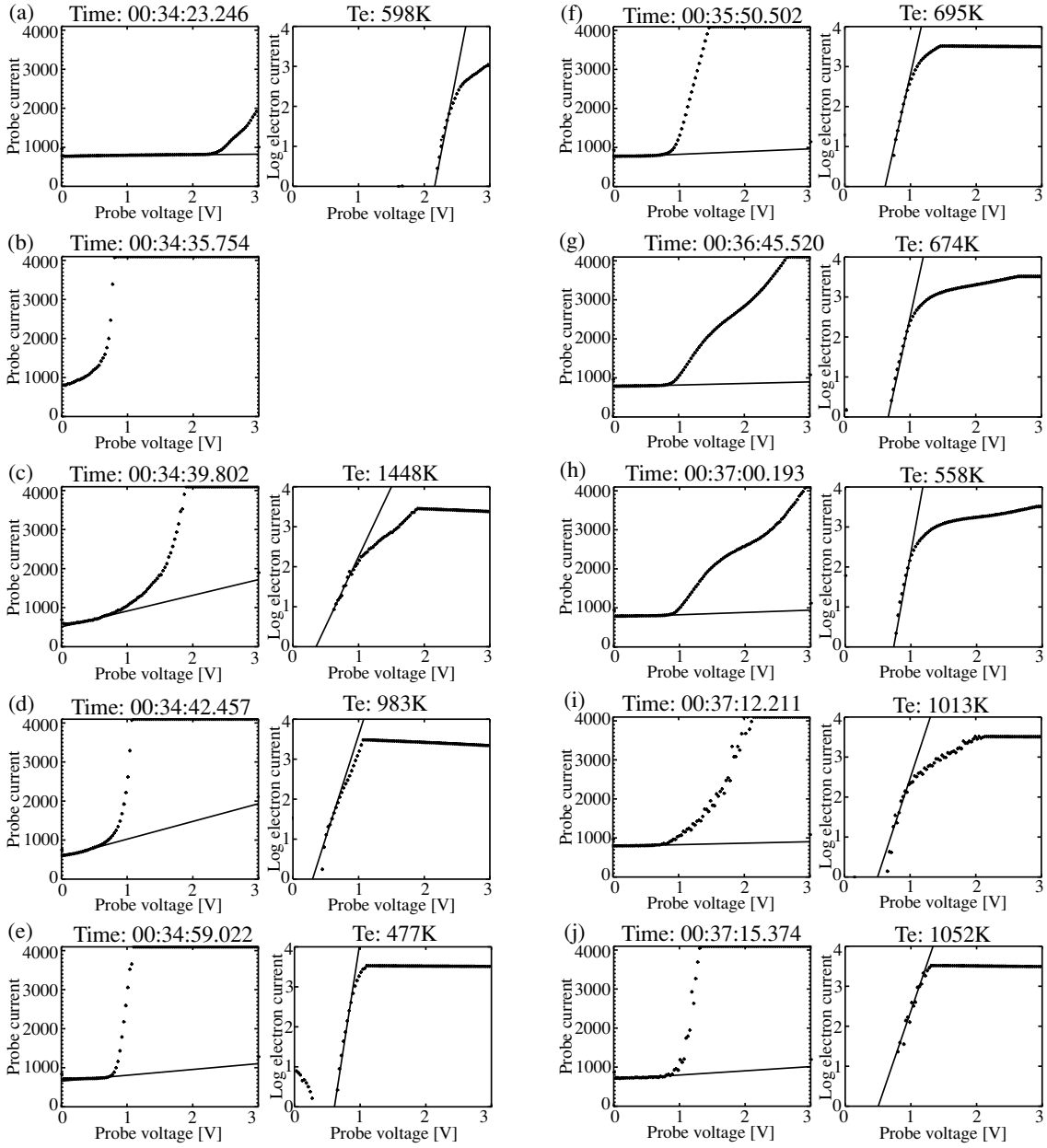

Fig. 1. Voltage versus current characteristics measured by the FLP instrument. The left row shows the probe current in a linear scale as a function of the probe bias together with the least squares fitting to the ion current, while the right one does the electron current in the logarithmic scale which was obtained by subtracting the ion current from the probe current.

density of molecular nitrogen (N_2), being based on the Electron Beam Fluorescence (EBF) technique (Kurihara *et al*., 2006), and thereby the rocket body was thought to be positively charged. On this condition, the passive plasma measurement such as Langmuir probe can be significantly interfered, and therefore reliable measurements can not be made. To avoid this interference, a payload zone of the rocket was separated into two stages; mother (a section close to the rocket motor) and daughter (an upper section). The FLP was installed on the mother stage together with other instruments (Abe *et al*., 2006), while the NTV was on the daughter stage. After separating the daughter from the mother stage at an altitude of 106.7 km, the passive measurements were expected to start a reliable measurement.

3. Observation

The sounding rocket "S-310-35" was launched from Andøya Rocket Range at 0:33 UT on Dec. 13, 2004. For the rocket trajectory, please refer to figure 1 of Kurihara *et al*. (2006). A time sequence prepared for the TED measurement described in Table 2 was executed during the rocket flight, i.e., the cylindrical probe started being deployed at 66 sec after the rocket launch (hereafter called X+66) and was completely exposed to the plasma outside the rocket sheath about 17 sec later (X+83) at an altitude of 92.7 km.

The left-side panel and right-side panel in Figs. 1(a)–(j) show the probe current as a function of the probe voltage (V-I characteristic curve) and the electron current in the logarithmic scale which was obtained by subtracting the ion current from the probe current, respectively. The linear

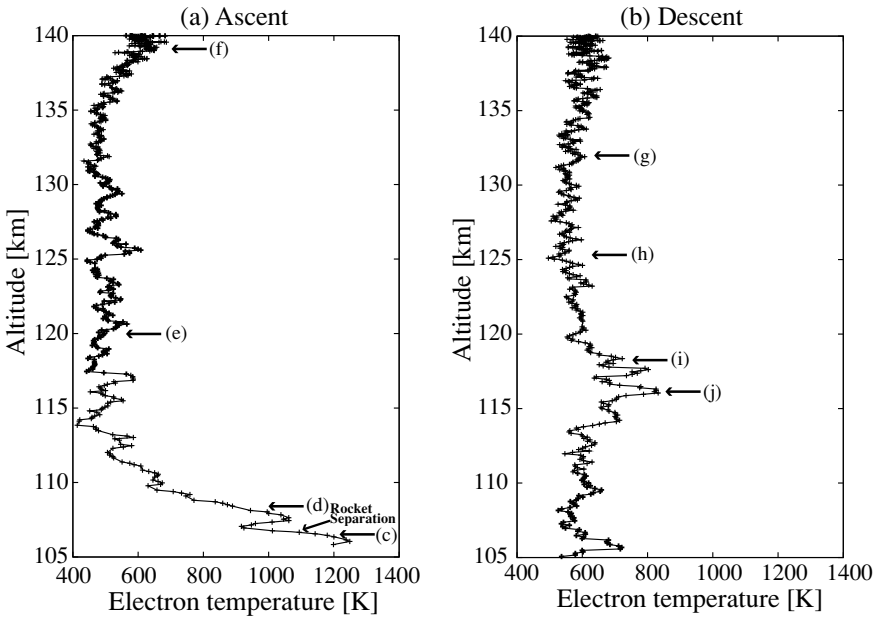

Fig. 2. Altitude profile of the electron temperature during the rocket (a) ascent and (b) descent. The characters (c)–(j) denote the altitudes where Figs. 1(c)–(j) were observed.

fitting to the ion current was represented by a thin line in the left panel. Shown at the top of the right panels are the electron temperatures calculated from the linear fitting to the electron current which increases exponentially. The V-I curve shown in Fig. 1(a) was obtained at X+83.2 sec, which corresponds to the time just after the probe was immersed in the ionospheric plasma.

At 00:34:29 UT (X+89), a high voltage power supply in the NTV instrument was turned on to emit a high-energy electron beam to excite a gas molecule by an inelastic collision with an electron (Kurihara *et al.*, 2006). In such a situation, the rocket was thought to be positively charged, although the actual potential depends on a balance between an amount of the emitted electron and that of the ambient thermal electrons incident on the rocket body. In fact, the V-I characteristic curves observed soon after X+89 were shifted in the negative direction beyond the lowest voltage of the probe bias, and thereat the electron temperature can not be calculated because it was impossible to identify an exponential variation of the electron current. This confirms that the rocket body was positively charged by the electron beam emission, because a voltage applied to the probe is given with reference to the rocket body.

At 00:34:35.8 UT, the V-I curve was again observed to appear in the range of the probe voltage sweep as shown in Fig. 1(b), suggesting that the rocket potential was moved to negative, and the electron temperatures were continuously estimated from the exponential part of the electron current for the rest part of the flight. We suppose that this potential change was caused by the intense electron precipitation and the resultant ionization, as will be discussed later. At 00:34:40 UT (X+100), the rocket was separated into two stages by strong springs at the joint part; daughter payload in the preceding stage and mother payload close to the rocket motor. After the separation, a potential of the mother stage was expected to be in the normal situation, because the NTV instrument that emits the electron beam was installed on the daughter stage while the FLP was on the mother stage.

Figures 1(d)-(j) show some of the V-I curves obtained for 3 minutes after the separation, while Fig. 1(c) is the one just before the separation. Since no significant changes in the rocket potential were detected all through the rest of the flight, it is easy to identify the ion current as well as electron current from which the electron temperatures are estimated. Figures 2(a) and (b) represent altitude profiles of the electron temperatures for the rocket ascent and descent, respectively. Each temperature is obtained by taking a running mean of 7 data points. The characters (c)–(j) denote the altitude where the V-I curves in Figs. 1(c)–(j) were obtained, respectively. As shown in Fig. 2(a), the estimated electron temperature is relatively high below 110 km altitude where the curves 1(c) and (d) were obtained. The temperature profile has a negative gradient, i.e., it decreases with altitude. The temperature shows insignificant change from 115 km to 135 km, whereas it slightly increases with altitude between 135 km and the apoapsis height of 140 km. On the other hand, the temperature profile during the descent in Fig. 2(b) has a different temperature structure, in which no obvious increases of the electron temperature were observed between 105 and 140 km. However, a small increase ($\sim$100–200 K) of the electron temperature against the background temperature was found to exist between 114 and 119 km altitude. It seems that the temperature peak is not single but multiple; local maxima at 118.4, 117.6, and 116.0 km.

During the rocket flight, the FLP sometimes detected unexpectedly high plasma density regions, where the electron saturation current exceeded the measurement range. When the space potential can not be determined from an inflection point in the V-I curve because of the saturation, it is not possible to make a reliable estimation of the electron number density in the Langmuir probe measurements. The reason

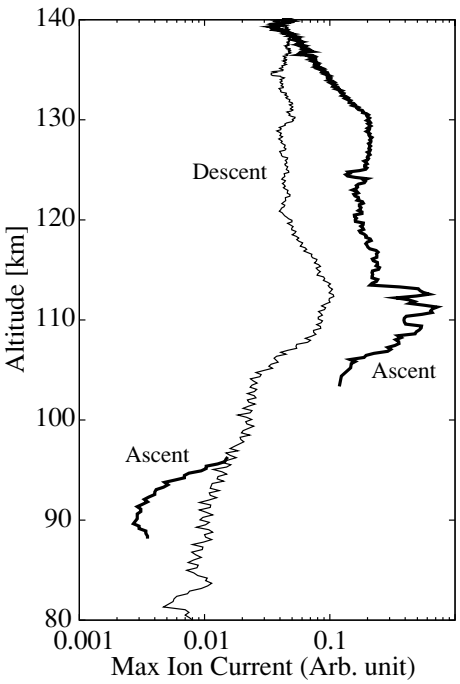

Fig. 3. Altitude profile of the maximum ion current in the V-I characteristics; Thick line: Ascent, Thin line: Descent.

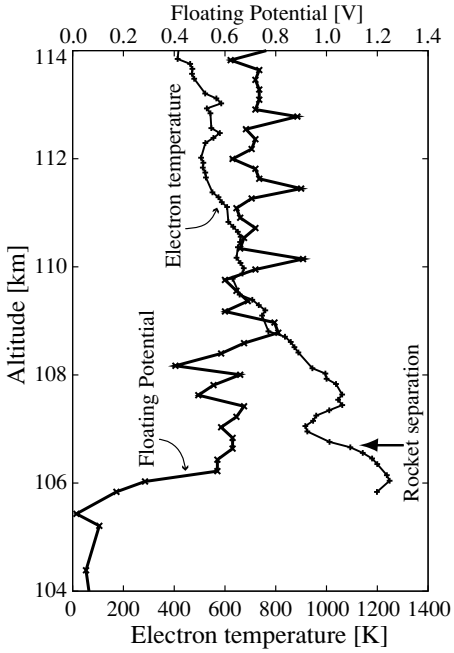

Fig. 4. Altitude profile of the floating potential and the electron temperature from the FLP measurement for the altitude range from 104 to 114 km.

for the current saturation seems not only the impact ionization by the precipitating electrons but the NTV originated electron beam might have contributed to some extent.

In order to understand overall tendency of the electron density variation, the maximum ion current in the V-I curve was used as a proxy. Figure 3 shows an altitude profile of the maximum ion current for both the ascending and descending flights. It was not possible to identify the ion current at altitudes between 96.3 km and 106.4 km during the ascent, because the rocket potential was severely charged to positive.

4. Discussion

4.1 Electron temperature increase at 106 km

The FLP observation shows a characteristic structure of the electron temperature during the ascending phase of the rocket flight. As shown in Fig. 2(a), the electron temperature profile has a local maximum of 1250 K at 106.0 km (X=99.3), immediately after the V-I curve started appearing in the range of the FLP sweep voltage at 105.8 km (X=99.0), where the rocket potential became ordinary for the first time since the NTV started emitting the electron beam at X=89.0. The precipitating electron data from the Auroral Particle Detector (APD) instrument (Ogasawara *et al.*, 2006) indicate that an enhancement of the precipitating electron flux was observed at X=98–99 and the large flux was continuously observed until X=115 (117.5 km). It is suggested from a comparison of the electron temperature with the APD data that this potential change was caused by the intense precipitating electron flux and the resultant ionization of neutral particles, because an increase of incident electrons can result in changing the potential into negative. Furthermore, such precipitating electrons can act as a heat source for the ambient electron gas through Coulomb collisions. A fraction of the incident auroral electron energy ultimately appears as electron gas thermal energy (see the review by Schunk and Nagy, 1978). However, heating rates due to the precipitating electrons are generally considered too low to explain the measured electron temperature enhancement.

Another possibility to explain the temperature increase in this region may be due to the artificial energetic electrons from the NTV instrument that generates electron beam with energy of about 1 keV, which is efficiently capable of ionizing neutral particles and is possible to eventually heat thermal electrons in the ambient plasmas. Thus, the electron beam may be, to some extent, responsible for the high electron temperatures. The detailed discussion of heating rates due to the NTV-originated electron beam should be made in the future.

4.2 Rocket potential variation

In order to confirm the above-described speculation about the rocket potential variation, the more quantitative evaluation has to be made. On the other hand, it is experimentally possible to know a temporal variation of the rocket potential by estimating the space potential in the V-I characteristic curve observed from the FLP. However, in unfavorable situation, very large number density of the electrons prevented us from identifying the space potential in the V-I curve. Therefore, a variation of the floating potential in the V-I curve is used as a proxy of the rocket potential. Note that an increase of the floating potential means a decrease of the rocket potential when assuming that the temperature and number density of the plasma are constant, because the former value is defined as a probe bias where the electron current is equal to the ion current, with reference to the later. Figure 4 shows variations of the floating potential of the FLP as well as the electron temperatures in

the altitude range of 104–114 km. As already explained, the floating potential suddenly increased by 0.5 V from 105.4 km to 106.2 km altitude while it remained less than 0.1 eV below 105.2 km. This is evidence that the rocket body was negatively charged just above this altitude. The exact coincidence of the time between the enhancement of precipitating electron flux from the APD and the start of a potential variation from the FLP just above 105.4 km (X=98) suggests that the rocket charging was caused by the precipitating electron and/or the resultant increase of thermal electron density. Above 106.2 km, the floating potential gradually increases up to 0.735 V at 114 km with a periodic variation caused by the rocket spinning modulation, i.e., the local maxima at 108.8, 110.1, 111.4, and 112.8 km were measured at the same direction in the rocket's spin plane, probably in a ram direction of the rocket velocity. In contrast, the variation between 106.2 and 108.7 seems unlikely periodical, and is probably attributed to a spatial structure.

The daughter payload was separated from the mother payload at X=100 (106.7 km), and thereafter the distance between the two payloads is expected to increase. The potential of the mother stage where the FLP was mounted was expected to change for the negative direction soon after the rocket separation at X=100 (106.7 km), because thereafter the electron beam emission from the daughter stage is no longer influential on the mother stage. Nevertheless, no significant variations were found in the rocket (mother) potential between before and after the separation. This suggests that the rocket potential was not affected by the NTV operation already at the time of separation but mainly determined by an amount of thermal electron flux incident on the rocket body. In other words, the incident thermal electron flux is obviously greater than the outward electron beam flux in this altitude range.

4.3 Electron temperature increase after the rocket separation

If the heating caused by the NTV-originated electrons was dominant, it would be weakened as the distance between the mother and the daughter increases. The decreasing trend of the temperature from 106.7 km to 107.2 km may be suggestive of such a relationship.

On the other hand, the electron temperature again increased with altitude above 106.7 km up to 107.6 km (see Fig. 4). The NTV-originated electrons tend to become less effective for the electron heating because the daughter stage was increasingly leaving from the mother. Instead, the precipitating electrons from higher altitudes may be considered as a more plausible source of the heating. In fact, the APD instrument successively observed the intense electron flux with energy larger than 3 keV (Ogasawara *et al.*, 2006) from X=98 (105.0 km) to X=115 (117.5 km). Figure 2(a) shows that the electron temperature profile has a decreasing trend up to an altitude of 114 km, while its gradient seems very small between 115 and 135 km altitude. As a general trend, the temperatures below 114 km are found to be higher than those above this altitude. The temporal correspondence between the precipitating electron flux enhancement and the high electron temperature implies that the electron heating is somehow related to the auroral electrons. However, the precipitating electrons are generally thought to cause electron temperature enhancements of only 20–50 K and totally inadequate to explain the measured electron temperature enhancement of up to 1000 K (Schlegel and St.-Maurice, 1981).

Observational evidence representing the existence of auroral arc near the rocket trajectory was found in the auroral emission distribution from optical observations in Kilpisjärvi, where all-sky camera was operated as one of the MIRACLE network during the DELTA campaign. The MIRACLE is a two-dimensional instrument network constructed for studies of mesoscale ionospheric physics in the Scandinavian sector (Syrjäsuo *et al.*, 1998). In Kilpisjärvi, the all-sky camera (ASC) acquires images through a filter of 557.7 nm with the sampling period of 20 sec. As shown in figure 1 of Kurihara *et al.* (2006), the discrete auroral arc was found to exist near the rocket trajectory at 00:34:40 UT (X=100) and 00:35:00 UT (X=120), and was observed to move toward the geophysical east direction. Lanchester *et al.* (1998) reported that large electric fields are present adjacent to auroral filaments produced by monoenergetic electron fluxes. Since no electric field measurements were made on the rocket, its actual existence can not be known. However, it may be possible that the high electron temperatures observed during the ascent may be caused by a modified two-stream instability created by the large electric fields.

During the DELTA campaign, the EISCAT radar was continuously operated at Tromsø, which is about 120 km far from the rocket launch site, and thereby the electric fields can be derived from observed ion velocity vector at 282 km as well as the electron temperature and density and ion temperature (Nozawa *et al.*, 2006). The EISCAT radar observations show that the southward electric field as large as 40 mV m^{-1} was present over Tromsø at the time of the rocket launch. Schlegel and St.-Maurice (1981) proposed that high-latitude E region electrons can be heated to substantial temperatures up to 1500 K in the presence of electric fields greater than 25 mV m^{-1}. Therefore, if the same magnitude of electric field as over Tromsø is present also near the rocket trajectory, the modified two-stream instability is probably responsible for the observed high electron temperatures.

4.4 Maximum ion current variation

The maximum ion current in the Langmuir V-I curve was considered to represent an overall trend of the plasma density variation, because it was not possible to estimate the electron number density during periods of high density situation. As shown in Fig. 3, the maximum current during the ascent is approximately a factor of 3 larger than that during the descent in general. The two profiles have a common bumpy structure around 110 km altitude; the maximum currents at 110 km for both phases are a factor of 3–4 larger than that in the surrounding region. Assuming that this maximum current increase is caused by the plasma density enhancement, the increase for the ascent is probably related to the electron precipitation, because the APD instrument actually observed the precipitating electrons. The precipitating electrons can cause both the ionization of neutral particles and the energization of thermal electrons. On the other hand, the dominant process for the high temperature region during the descent is likely different from the parti-

cle heating, because it is suggested that the thermal electron heating rate has the maximum value at altitudes higher than the most effective ionization layer; the local temperature increase was observed to be at altitudes between 114 and 119 km while the profile of the maximum ion current has a peak at ∼113 km altitude. It will be necessary to discuss the maximum ion current variation together with the electron density and ion temperature both of which can be derived from the EISCAT radar observations (Nozawa *et al.*, 2006).

4.5 Electron temperature variation during the descent

The electron temperature profile observed during the rocket descent has a rather monotonic trend, in which no significant gradient with altitude was found except that it locally increased by about 100–200 K at altitudes between 114 (X=258.6) and 119 (X=251.2) km. Such a local variation may be reflected by not a vertical temperature structure but a horizontal one. In general, a temperature variation along the magnetic line of force is much less than in the transverse direction. When one considers that the rocket was moving across the magnetic field direction, it may be possible for the rocket to traverse a region of higher electron temperature at the altitude between 114 and 119 km.

The V-I characteristic curves as in Figs. 1(g)–(j) confirm that the least squares fitting for the temperature estimation was made with accuracy, although a small deviation of the points from the least squares fitting seems to exist for the curves in Figs. 1(i) and (j) for which higher electron temperatures were estimated. A fact that no precipitating electrons were observed in the APD instruments for the period from X=251.2 and 258.6 denies its causal relationship with the particle heating. There still remains a possibility of the heating by precipitating electrons whose energy is too low (<3 keV) for the APD to be detected and the related heat conduction along the magnetic field lines. However, the auroral images taken by the all-sky camera in Kilpisjärvi suggest that no auroral emission was found to exist near the rocket trajectory during the descending phase (see figure 1 of Kurihara *et al.*, 2006).

Another possible mechanism for the electron temperature increase may be due to heating from the Farley-Buneman instability (Farley, 1963; Buneman, 1963) in the presence of strong electric field. When the amplitude of the convection electric field exceeds a threshold value of $E \simeq 20$ mV/m in the high-latitude E region, the Farley-Buneman instability may be developed. This instability results in a broadband turbulent electric field, coupled with plasma density perturbations (Farley, 1963; Buneman, 1963). St.-Maurice *et al.* (1981) and St.-Maurice and Schlegel (1982) interpreted the temperature enhancements as a heating of the electron gas by unstable waves excited by the modified two-stream or Farley-Buneman plasma instability. In their numerical approach, St.-Maurice and Schlegel (1982) introduced a free parameter to describe the heating, namely the relative amplitude $\delta N/N$ of the density fluctuations. They found a reasonable agreement between their calculations and the measured electron temperature with values of 2–4% for $\delta N/N$ quoted in the literature. Also on the Porcupine II sounding rocket experiment, electron density fluctuations ($\delta N/N$) with a ratio of 2–5% were observed to exist, together with intense electrostatic waves, in the unstable auroral electrojet region (Pfaff *et al.*, 1984).

In our measurements, a remarkable scattering in the probe current can be seen in Figs. 1(i) and (j), and which may be evidence of small-scale plasma density perturbations. A spectrum analysis of the probe currents suggests that the perturbation has a relatively stronger power in the spatial scale of 1–10 meters. The relative amplitude ($\delta N/N$) is estimated to be about 4–6%, when the probe current is assumed to be proportional to the electron density. These numbers seem to be larger than mean density fluctuation level of 2–4% inferred from Chatanika radar measurements described in St.-Maurice and Schlegel (1982). However, they also indicated that the perturbed density level has to be larger when the amplitude of the electric field is smaller. In the previous observational studies dealing with the Farley-Buneman instability, the electron temperature estimation was mostly based on radar measurements, while the density perturbation was detected by *in-situ* plasma probe. In the E-region Rocket/Radar Instability Study (ERRRIS), two of the three rockets equipped with swept Langmuir probe as well as d.c. electric field probe, magnetometer and other instruments encountered intense two-stream waves in the unstable electrojet (Pfaff *et al.*, 1992). However, no electron temperature data were reported from these observations, while highly variable d.c. electric fields were identified in this region. In contrast, our observation is, to our knowledge, the first time that both the temperature increase and density fluctuation were detected by *in-situ* observation on the sounding rocket.

Further study will be needed to clarify how the two-stream or Farley-Buneman instability causes such a temperature increase by conducting a numerical simulation with the ground-based magnetometer data as well as electric field, ion and electron temperature data from the EISCAT observations.

5. Summary

From the Fast Langmuir Probe (FLP) observations on board the sounding rocket "S-310-35" during the Dynamics and Energetics of the Lower Thermosphere in Aurora (DELTA) campaign, we successfully measured the electron temperatures in the high-latitude lower ionosphere. The obtained temperature profiles indicate that the ionospheric thermal structure was greatly affected by the auroral energy input. There still remains a possibility that one of the accompanying instruments on the rocket may artificially exert an influence on the local electron temperature. The results of our study are summarized as follows:

1) The electron temperatures observed during the rocket ascent were found to be remarkably high below 114 km altitude. The lowest part (<107.2 km) of such a high temperature region may partly be attributed to artificial electron beam generated by the N_2 temperature instrument on the same rocket, while the remaining part of the high temperatures above 107.2 km reflects a real variation of the ionospheric thermal structure.
2) From a comparison of the rocket measurements with the All-Sky Camera observations, it should be noted that the discrete auroral arc was located near the rocket

trajectory when the temperature enhancements were observed at an altitude from 107 to 114 km during the rocket ascent. The higher electron temperatures may be attributed to the Farley-Buneman instability caused by the large electric fields, which are often present adjacent to auroral arc produced by the precipitating electrons.

3) A small increase (∼100–200 K) of the electron temperature observed at the altitude of 114–118 km during the rocket descent is unlikely to have been caused by particle heating since no precipitating electrons were observed onboard the rocket during the corresponding interval. In this event as well, the Farley-Buneman instability may be a possible heating mechanism. The small-scale electron density perturbations estimated from the I-V characteristics of the langmuir probe on the rocket substantiates this assumption. To our knowledge, this is the first *in-situ* observation of both the temperature increase and density perturbation that may be caused by the Farley-Buneman instability.
4) The V-I curves measured by the FLP indicate that the rocket potential was affected by various factors; the ambient electron density, the electron beam emitted by the NTV instrument, the precipitating electrons and the resultant increase of electron density. The potential variation is qualitatively explainable by considering inward and outward flux of electrons to the rocket body.

Acknowledgments. We are very grateful to all the staff of ISAS (Institute of Space and Astronautical Science) and ARR (Andøya Rocket Range) for the rocket launch. Thanks are also due to all the staff of the ground-based observations during the DELTA campaign. We are also indebted to Drs. K. Kauristie and Y. Ogawa for their contribution to provide all-sky camera images. This work was carried out by the joint research program of the Solar-Terrestrial Environment Laboratory, Nagoya University.

References

Abe *et al.*, Dynamics and Energetics of the Lower Thermosphere in Aurora (DELTA) —Japanese sounding rocket campaign—, *Earth Planets Space*, **58**, this issue, 1165–1171, 2006.

Banks, P. M., Observations of joule and particle heating in the auroral zone, *J. Atmos. Terr. Phys.*, **39**, 179–193, 1977.

Banks, P. M. and C. R. Chappell, A new model for the interaction of auroral electrons with the atmosphere: Spectral degradation, backscatter, optical emission, and ionization, *J. Geophys. Res.*, **79**, 1459–1470, 1974.

Brace, L. H., Langmuir probe measurements in the ionosphere, in *Measurement Techniques in Space Plasmas: Particles*, edited by R. F. Pfaff, J. E. Borovsky, and D. T. Young, pp. 23–35, American Geophysical Union Monograph 102, 1998.

Brekke, A., Joule heating and particle precipitation, *Adv. Space Res.*, **2**, 45–53, 1983.

Buneman, O., Excitation of field-aligned sound waves by electron streams, *Phys. Rev. Lett.*, **10**, 285–287, 1963.

Farley, D. T., A plasma instability resulting in field-aligned irregularities in the ionosphere, *J. Geophys. Res.*, **68**, 6083–6097, 1963.

Kurihara, J., T. Abe, K. I. Oyama, E. Griffin, M. Kosch, A. Aruliah, K. Kauristie, Y. Ogawa, S. Komada, and N. Iwagami, Observations of the lower thermospheric neutral temperature and density in the DELTA campaign, *Earth Planets Space*, **58**, this issue, 1123–1130, 2006.

Lanchester, B. S., M. H. Rees, K. J. F. Sedgemore, J. R. Palmer, H. U. Frey, and K. U. Kaila, Ionospheric response to variable electric fields in small-scale auroral structures, *Ann. Geophys.*, **16**, 1343–1354, 1998.

Larsen, M. F., T. R. Marshall, I. S. Mikkelsen, B. A. Emery, A. Christensen, D. Kayser, J. Hecht, L. Lyons, and R. Walterscheid, Atmospheric Response in Aurora experiment: Observations of E and F region neutral winds in a region of postmidnight diffuse aurora, *J. Geophys. Res.*, **100**, 17299–17308, 1995.

Larsen, M. F., A. B. Christensen, and C. D. Odom, Observations of unstable atmospheric shear layers in the lower E region in the post-midnight auroral oval, *Geophys. Res. Lett.*, **24**, 1915–1918, 1997.

Nozawa, S., Y. Ogawa, A. Brekke, T. Tsuda, C. M. Hall, H. Miyaoka, J. Kurihara, T. Abe, and R. Fujii, EISCAT observational results during the DELTA campaign, *Earth Planets Space*, **58**, this issue, 1183–1191, 2006.

Ogasawara, K., K. Asamura, T. Takashima, Y. Saito, and T. Mukai, Rocket observation of energetic electrons in the low-altitude auroral ionosphere during the DELTA campaign, *Earth Planets Space*, **58**, this issue, 1155–1163, 2006.

Oyama, K. I. and K. Hirao, Application of a glass-sealed Langmuir probe to ionospheric study, *Rev. Sci. Instruments*, **47**, 101–107, 1976.

Pfaff, R. F., M. C. Kelley, B. G. Fejer, E. Kudeki, C. W. Carlson, A. Pedersen, and B. Hausler, Electric field and plasma density measurements in the auroral electrojet, *J. Geophys. Res.*, **89**, 236–244, 1984.

Pfaff, R. F., J. Sahr, J. F. Providakes, W. E. Swartz, D. T. Farley, P. M. Kintner, I. Haggstrom, A. Hedberg, H. Opgenoorth, and G. Holmgren, The E-region Rocket/Radar Instability Study (ERRRIS)—Scientific objectives and campaign overview, *J. Atmos. Terr. Phys.*, **54**(6), 779–808, 1992.

Schlegel, K. and J. P. St.-Maurice, Anomalous heating of the polar E region by unstable plasma waves 1. Observations, *J. Geophys. Res.*, **86**, 1447–1452, 1981.

Schunk, R. W. and A. F. Nagy, Electron temperatures in the F region of the ionosphere—Theory and observations, *Rev. Geophys.*, **16**, 355–399, 1978.

St-Maurice, J. P., Electron heating by plasma waves in the high latitude E-region and related effects: Theory, *Adv. Space Res.*, **10**(6), 239–249, 1990.

St.-Maurice, J. P. and K. Schlegel, Estimates of plasma wave amplitudes in the turbulent high-latitude E region using electron temperature measurements, *J. Geophys. Res.*, **87**, 5197–5201, 1982.

St.-Maurice, J. P., K. Schlegel, and P. M. Banks, Anomalous heating of the polar E region by unstable plasma waves 2. Theory, *J. Geophys. Res.*, **86**, 1453–1462, 1981.

Syrjäsuo, M. T., T. I. Pulkkinen, R. J. Pellinen, P. Janhunen, K. Kauristie, A. Viljanen, H. J. Opgenoorth, P. Karlsson, S. Wallman, P. Eglitis, O. Amm, E. Nielsen, and C. Thomas, Observations of substorm electrodynamics using the MIRACLE network, *Proceedings of the International Conference on Substorms-4*, edited by S. Kokubun and Y. Kamide pp. 111–114, Astrophysics and Space Science Library, vol. 238, Terra Scientific Publishing Company, Kluwer Academic Publishers, 1998.

T. Abe (e-mail: abe@isas.jaxa.jp), K. Oyama, and A. Kadohata